

## Detection of Cochlear Amplification and Its Activation

Wei Dong<sup>†</sup> and Elizabeth S. Olson<sup>†‡\*</sup>

<sup>†</sup>Otolaryngology, Head and Neck Surgery and <sup>‡</sup>Biomedical Engineering Columbia University, New York, New York

### 1. Background for BM displacement analysis

The Navier-Stokes equation relates pressure gradients to fluid motion in an incompressible fluid:

$$\nabla p = -\rho \frac{\partial \mathbf{v}}{\partial t} - \rho \mathbf{v} \cdot \nabla \mathbf{v} + \mu \nabla^2 \mathbf{v}. \quad \rho \text{ is fluid density, assumed that of water, } 10^3 \text{ kg/m}^3. \quad \mu \text{ is the}$$

viscosity of the perilymph, taken as that of water,  $10^{-3} \text{ kg/(m}\cdot\text{s)}$ .  $\mathbf{v}$  is the fluid velocity (m/s). The sizes of the terms in the Navier-Stokes equation that involve fluid velocity can be estimated using dimensional analysis. Define  $L$  and  $U$ , scale factors used to characterize the fluid system.  $L$  is the extent over which fluid velocities vary by a factor of  $e$ , and was found in (1) to be  $\sim 15 \mu\text{m}$ , independent of stimulus level and frequency.  $U$  is the velocity of the BM.  $U$  depends on frequency and SPL. At the BF (24 kHz) it is  $\sim 0.5 \text{ mm/s}$  at 30 dB SPL and  $\sim 3 \text{ mm/s}$  at 80 dB SPL. At 5 kHz it is  $\sim 2 \mu\text{m/s}$  at 30 dB SPL and  $\sim 0.6 \text{ mm/s}$  at 80 dB SPL.  $\omega$  is radian frequency. In the table S1 below we compare the estimated sizes of the three terms that depend on fluid velocity.

Freq & Level	$\rho \frac{\partial \mathbf{v}}{\partial t} \Rightarrow \rho U \omega$	$\rho \mathbf{v} \cdot \nabla \mathbf{v} \Rightarrow \frac{\rho U^2}{L}$	$\mu \nabla^2 \mathbf{v} \Rightarrow \frac{\mu U}{L^2}$
24kHz 30dB	75000	17	2200
24kHz 80dB	450000	600	13000
5kHz 30dB	63	.0003	9
5kHz 80dB	19000	24	2700

**Table S1 Comparison of three terms in the Navier-Stokes equation depending on fluid velocity**

The second (nonlinear) term is much smaller than the other terms in all entries. The first (inertial) term is larger than the last (viscous) term by a factor of 34 at 24 kHz and a factor of 7 at 5 kHz. Thus, the Navier-Stokes equation can be approximated as  $\nabla p = -\rho \frac{\partial \mathbf{v}}{\partial t}$  for frequencies above 5 kHz.

### 2. Characteristics of wire electrode frequency response

The frequency response of our wire electrode was characterized following the method cited in (2, 3). The result is in the plot below (green in Fig. S1). For comparison we include the frequency response of a glass electrode of similar impedance (magenta in Fig. S1). Both electrodes had impedances slightly under 1 M-Ohm when measured at 500 Hz. The frequency response of the wire electrode is broad-band. The glass electrode has much steeper low-pass filtering. (At high frequencies the response from the glass electrode deviates from a low-pass filter, likely due to capacitive coupling.) Because the  $\sim 1.5 \mu\text{m}$  isonel coating of the wire,

although thin, is much thicker than the glass thickness at the tip of a glass electrode, the capacitance is much smaller. Also, the resistance of platinum is much less than that of even concentrated saline. Thus, the RC time constant of our plastic-coated platinum electrode is much smaller than that of a pulled glass electrode. Also included in the plot is the frequency response of one of our micro-pressure sensors (blue dashed line in Fig. S1, the sensor used in wg165, our highlighted experiment; the calibration shown was done at the end of data collection). The sensor was calibrated using a shaker with attached accelerometer, a method from the literature and described in (4). (Structure evident in the sensor calibration is related to imperfections in the motion of the shaker, since such structure is typically present in all sensors calibrated at the same time.) Both the sensor and wire electrode, with their associated electronics, are broad-band with mild low-pass filtering (Fig. S1A). Their phase change with frequency was small and their relative phase was for our purposes negligibly small (Fig. S1B). Thus no correction between their relative phases was applied.

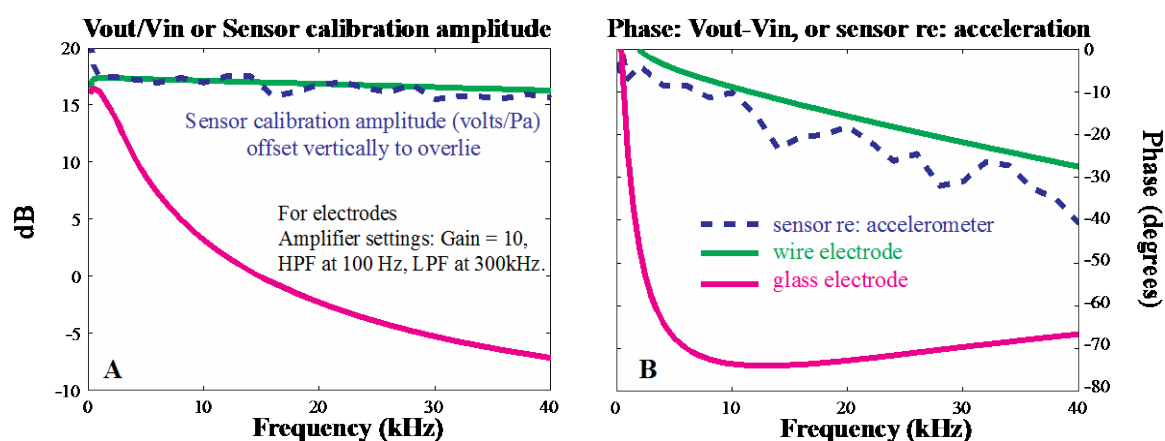


Fig. S1 Comparison of frequency responses among wire electrode, glass electrode and pressure sensor. (A) Amplitude; (B) Phase.

### 3. Negative resistance confirmation

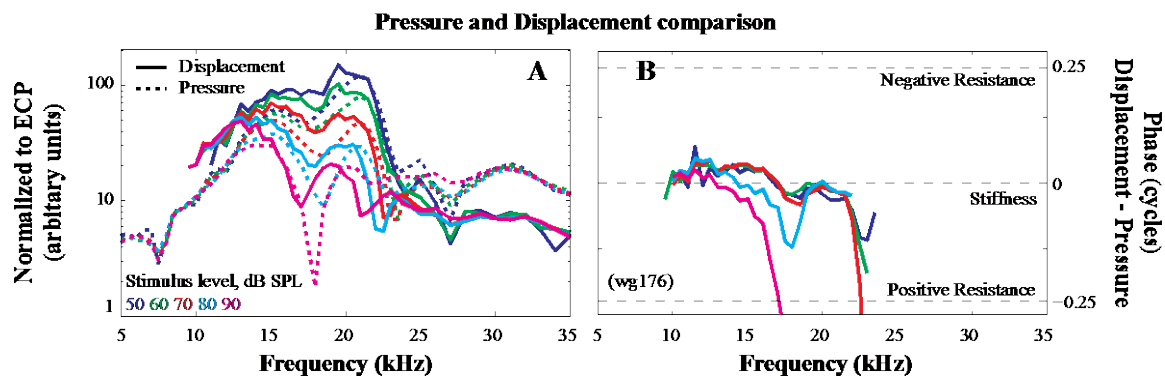
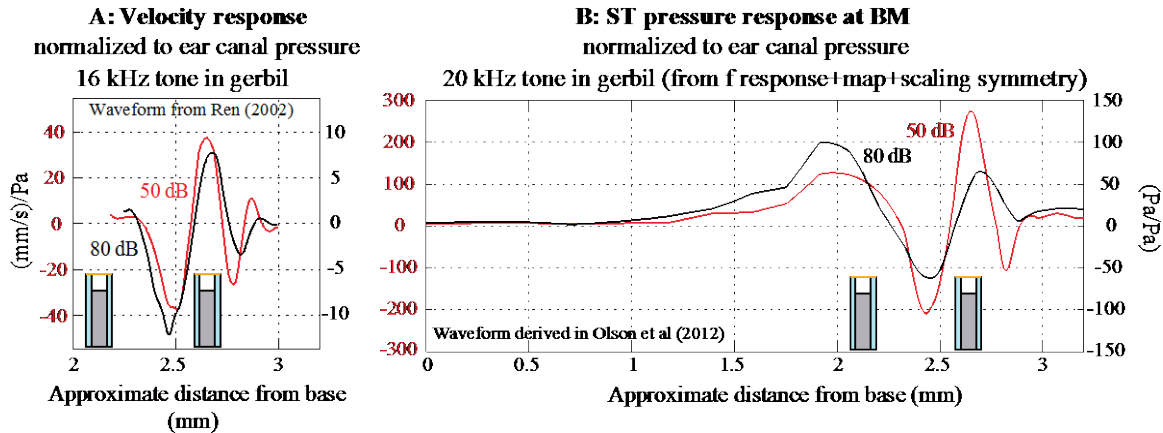


Fig. S2 Comparison of pressure and displacement in preparation wg176.

(A) Amplitude normalized to ear canal pressure; (B) Relative phase. Sound stimulation was 50 - 90 dB in 10 dB steps. Pressure sensor positioned  $\sim 10 \mu\text{m}$  from the BM for pressure (dotted lines in A) and 10 - 20  $\mu\text{m}$  for BM displacement calculation (solid lines in A). (wg176)

In Fig. 4B we showed that the phase of displacement led the pressure slightly in the compressively nonlinear frequency region, evincing negative resistance and power gain. Fig. S2 confirms the finding by showing negative resistance in another active preparation (wg176). The pressure sensor was positioned 10  $\mu\text{m}$  from the BM for the pressure measurement, 10 and 20  $\mu\text{m}$  for the BM displacement measurement. In phase, displacement led pressure slightly in the frequency region where responses were compressively nonlinear. This phase evinces negative resistance and thus power gain, and confirmed the results from wg165.

#### 4. Resolution of pressure measurements.



**Fig. S3 Time waveform from velocity and pressure measurements**

(A) Waveform of BM velocity (re-plotted from (5)). (B) Waveform of ST pressure near the BM (re-plotted from (6)). Red and black represent the responses at 50 and 80 dB SPL. Schematic pressure sensor diameter was scaled relative to the wavelength of cochlear traveling wave in each panel.

Pressure sensor diameter is shown to-scale relative to wavelength of cochlear traveling wave. Waveform of basilar membrane velocity is in Fig. S3A, from (5). Waveform of scala tympani pressure near the basilar membrane is in Fig. S3B, found with frequency response data coupled to the cochlear map and employing the concept of scaling symmetry (6). Based on these figures, when measuring at frequencies near the BF of the sensor location, the sensor membrane spans  $\sim 1/4$  wave and when measuring at frequencies 0.5 octave lower than the BF of the sensor location, for which the wave peaks  $\sim 0.5$  mm further apical, the sensor membrane spans less than 0.1 wave. Thus, sensor resolution is reasonable. These figures also show that near the best place the wavelength increases with SPL about 10% from 50 – 80 dB SPL.

#### References:

1. Olson, E.S. (1999) Direct measurement of intra-cochlear pressure waves. *Nature* 402(6761):526-529.
2. Fridberger, A., *et al.* (2004) Organ of Corti potentials and the motion of the basilar membrane. *The Journal of neuroscience : the official journal of the Society for Neuroscience* 24(45):10057-10063.
3. Baden-Kristensen, K. & T.F. Weiss (1983) Receptor potentials of lizard hair cells with free-standing stereocilia: responses to acoustic clicks. *The Journal of physiology* 335:699-721.

4. Olson, E.S. (1998) Observing middle and inner ear mechanics with novel intracochlear pressure sensors. *The Journal of the Acoustical Society of America* 103(6):3445-3463.
5. Ren, T. (2002) Longitudinal pattern of basilar membrane vibration in the sensitive cochlea. *Proceedings of the National Academy of Sciences of the United States of America* 99(26):17101-17106.
6. Olson, E.S., H. Duifhuis, & C.R. Steele (2012) Von Bekesy and cochlear mechanics. *Hearing research* 293(1-2):31-43